

Deep learning based diagnosis of PTSD using 3D-CNN and resting-state fMRI data

Mirza Naveed Shahzad^{*}, Haider Ali

Department of Statistics, University of Gujrat, Gujrat, Pakistan



ARTICLE INFO

Keywords:

PTSD
rs-fMRI
Machine Learning techniques
ICA
3D-CNN
k-fold cross-validation

ABSTRACT

Background: The incidence rate of Posttraumatic stress disorder (PTSD) is currently increasing due to wars, terrorism, and pandemic disease situations. Therefore, accurate detection of PTSD is crucial for the treatment of the patients, for this purpose, the present study aims to classify individuals with PTSD versus healthy control.

Methods: The resting-state functional MRI (rs-fMRI) scans of 19 PTSD and 24 healthy control male subjects have been used to identify the activation pattern in most affected brain regions using group-level independent component analysis (ICA) and *t*-test. To classify PTSD-affected subjects from healthy control six machine learning techniques including random forest, Naive Bayes, support vector machine, decision tree, K-nearest neighbor, linear discriminant analysis, and deep learning three-dimensional 3D-CNN have been performed on the data and compared.

Results: The rs-fMRI scans of the most commonly investigated 11 regions of trauma-exposed and healthy brains are analyzed to observe their level of activation. Amygdala and insula regions are determined as the most activated regions from the regions-of-interest in the brain of PTSD subjects. In addition, machine learning techniques have been applied to the components extracted from ICA but the models provided low classification accuracy. The ICA components are also fed into the 3D-CNN model, which is trained with a 5-fold cross-validation method. The 3D-CNN model demonstrated high accuracies, such as 98.12%, 98.25 %, and 98.00 % on average with training, validation, and testing datasets, respectively.

Conclusion: The findings indicate that 3D-CNN is a surpassing method than the other six considered techniques and it helps to recognize PTSD patients accurately.

1. Introduction

Posttraumatic stress disorder (PTSD) is one of the most common mental health disorders. This chronic and debilitating disorder can occur after a particularly distressing or threatening life event, such as a natural disaster, military combat, unexpected loss of a loved one, or sexual assault or traffic accidents (Watkins et al., 2018; Z Zhu et al., 2023). It is characterized by symptom clusters such as avoidance, re-experiencing the trauma memories, hyperarousal, and negative cognitions (Ke et al., 2016). The typical symptoms of PTSD persevere over a long period and the prevalence of PTSD in most studies is reported up to 30 %, after a natural disaster (Zhu et al., 2020). At least 7 % of people from the general population fulfill the occurrence criteria of PTSD at some time in their lives (Kessler et al., 2005). PTSD is a debilitating psychiatric disorder that is associated with problems including physical health problems, social dysfunction, and difficulties at work (Galovski

and Lyons, 2004; Investigators et al., 2004; Smith et al., 2005). Timely and accurate diagnosis of PTSD is more important for the treatment. Normally, the PTSD diagnosis relies on self-reporting of symptoms. However, there has been increased interest in identifying objective biomarkers of PTSD to facilitate diagnosis. Functional magnetic resonance imaging (fMRI) is a highly effective method to collect brain activation data (Norman et al., 2006). And resting-state fMRI (rs-fMRI) data are very advantageous in the investigation of clinical populations, memory functions, mental status, and the functional relationships between different brain areas (Shirer et al., 2012), for more details, see Fox and Greicius (Fox and Greicius, 2010). This study also obtained the rs-fMRI scans to identify the activation pattern in the brain of PTSD subjects.

In this regard, previous large-scale studies have employed functional neuroimaging, particularly fMRI. The fMRI is a powerful tool used extensively in research to analyze activation in the brain (Logothetis,

* Corresponding author.

E-mail address: nvd.shzd@uog.edu.pk (M.N. Shahzad).

2008). The goal of fMRI investigations is to explore and understand the neural systems and processes underlying several cognitive functions, behavioral patterns, emotional responses, sensory perception, motor control, and speech processing (Bandettini, 2012; Yen et al., 2023). There are two types of fMRI studies, resting state fMRI (rs-fMRI) and task-based fMRI. But, rs-fMRI has become a popular alternative technique for examining brain function models for psychological disorders and it has many advantages over task-based fMRI (Canario et al., 2021). To diagnose PTSD, researchers have increasingly turned to rs-fMRI (X Zhu et al., 2023), and several studies using rs-fMRI data have linked abnormalities to the insula, amygdala, Anterior Cingulate Cortex (ACC), hippocampus, Medial Pre-frontal Cortex (MPFC), thalamus, prefrontal cortex, parahippocampus, and other brain regions (Bruce et al., 2013; Francati et al., 2007; Hughes and Shin, 2011). However, there is inconsistency observed regarding affected areas of the brain involved with PTSD, even conflict in other investigations about the hyperactivation and hypoactivation brain areas (Christova et al., 2015). Nevertheless, the findings come mainly from comparing structural numerical data of PTSD patients with a group of healthy individuals.

To date, in studies attempting the classification of PTSD, visual data investigations have been rarely found. In the past few years, the application of deep learning techniques such as Convolutional Neural Networks (CNN) to neuroimaging has made promising improvements in brain disease classification (Sivaranjini and Sujatha, 2020; Abbas et al., 2023; Agarwal et al., 2023). A rising number of research have recently used neuroimaging data to identify psychiatric disorders using machine learning and deep learning techniques (Chen et al., 2020; Liu et al., 2015). However, hardly found studies that used 3D-CNN in the analysis of PTSD neuroimaging data. However, ICA has been applied to fMRI data to find out the functional connectivity using rs-fMRI data, because it gives a more detailed and informative network analysis (Dipasquale et al., 2015). In fMRI data analysis, the application of ICA enables effective data preparation, noise reduction, feature extraction, dimensionality reduction, and enhanced analysis accuracy of brain activity patterns. This data-driven technique decomposes fMRI data into spatially independent components to separate noise more appropriately (Oh et al., 2017), identify functional connectivity patterns (Dipasquale et al., 2015), capture the most salient information, and enhance the detection of relevant brain activation patterns (Oh et al., 2017). It improves the performance of machine learning algorithms. In separating patients with schizophrenia from normal controls, (Qureshi et al., 2017) attained the highest classification accuracy using the ICA features.

After applying ICA to improve the quality of the data and interpretability of brain activity patterns, 3D-CNNs can efficiently learn and analyze the spatial and temporal characteristics of the data. CNN is an outstanding statistical deep-learning approach for classification including images, object recognition, image retrieval, and image generation (Jiao et al., 2018). It includes pooling, normalization, and fully connected layers in its network structure. In a 3D-CNN, the pooling layer performs downsampling, helps achieve translation invariance, builds spatial hierarchies, boosts parameter efficiency, and improves noise robustness. The normalization layer aids in a variety of tasks, including regularizing the network, handling varied scales, expediting training, enhancing generalization, and normalizing activations. When analyzing and extracting significant features from 3D data, these functions help the network to be stable, effective, and performing. In the normalization layer, an element activation function applies such as the $\max(0, x)$ thresholding zero which does not change the size of the image. We have designed a 3D-CNN model to classify the PTSD brain images that were generated from the ICA method. The hybrid approach of 3D-CNN with the ICA method using rs-fMRI scans has been used to improve the performance and accuracy rate of the study. The ICA-based 3D-CNN model performance measure with accuracy, loss, area under the curve (AUC) with 95 % confidence interval (CI) of AUC, sensitivity, specificity, False Negative rate (FNR), false positive rate (FPR), precision and confusion matrix. We have employed 3D ICA data as input data for the 3D-CNN

model to classify PTSD and healthy control participants for the first time in the present work, making it unique in the field.

2. Methodology

The primary objective of this study is twofold: first, to explore the activation pattern in brain regions in the individuals who have been diagnosed with PTSD as compared to the control group; and second, to develop an ICA-based 3D-CNN model. The ultimate objective is to accurately classify the individuals with PTSD and healthy controls using the developed model and rs-fMRI scans. Our research goals have been achieved through two distinct phases, after the data acquisition and preprocessing. The data is preprocessed using the standard preprocessing steps for the fMRI data, for the details of the standard preprocessing steps, we refer to the studies (Nichols et al., 2017), (Sladky et al., 2011), and Mikl et al. (Mikl et al., 2008). In the first phase, best ICA components are obtained by applying group-level ICA and two-sample t-test was sued to obtain the activation pattern, and in the second phase, 3D-CNN deep learning is utilized for classification purposes.

2.1. Data acquisition and preprocessing

A recent large fMRI study conducted by the Department of Defense (DoD) Alzheimer's Disease Neuroimaging Initiative (ADNI) on elderly Vietnam Veterans and healthy controls, the detailed description of the study explained by (Weiner et al., 2017) This dataset data utilized in the present study, and obtained the rs-fMRI scans of the 19 PTSD and 24 healthy control male subjects, those are on average 70.56 and 73.74 years old, respectively. Some more demographic information about the subjects is provided in Table 1. Additionally, the rs-fMRI (open eyes) scans obtained of both cases, which had 140 brain images and 48 slices with an axial view more as scans had properties like field strength = 3.0 tesla, flip angle = 90.0°, manufacturer = GE medical systems, matrix X = 64.0 pixels, matrix Y = 64.0 pixels, mfg Model = discovery mr750, pixel spacing X = 3.2813 mm, pixel spacing Y = 3.2813 mm, pulse sequence = EP/GR, slices = 5952.0, slice thickness = 3.2999 mm, TE = 30.0 ms and TR = 2900.0 ms.

The raw rs-fMRI images were preprocessed with SPM12. The standard preprocessing steps applied on raw scans for motion correction, slice time correction, realignment, normalization, and smoothness with a 6 mm full-width half-maximum Gaussian kernel. The slice time correction is used to correct the temporally misaligned slices. The realignment step has been taken to correct head motion and ensure that the brain's position is consistent across all functional scans. As the human brain size varies among individuals, a standard procedure of normalization method is used to normalize the rs-fMRI scans.

Table 1
Demographic information of subjects.

Groups	PTSD	Healthy Control
Subjects Count	19	24
Gender/ Participant	Male/Veteran of the Vietnam War	Male/Veteran of the Vietnam War
Age group	70–75	70–75
Average Age	70.56	73.7
Scans type	Axial Resting-State fMRI	Axial Resting-State fMRI
Eyes Open	Yes	Yes
Pre/Post processing	Axial(x)= 64/75, Sagittal(y)= 64/95, coronal(z)= 48/79	Axial(x)= 64/75, Sagittal(y)= 64/95, coronal(z)= 48/79
Exclusion criteria	CAPS score<50, MCI/ Dementia, Loss of Consciousness for >5 min	CAPS score>30, MCI/ Dementia, Loss of Consciousness for >5 min

CAPS= Clinician-Administered PTSD Scale, MCI= Mild Cognitive Impairment.

2.2. Components selection and activation analysis by group-level ICA and t-test

Independent Component Analysis (ICA) is a powerful data-driven technique. It is frequently utilized in rs-fMRI studies to attain functional connectivity patterns and to study how different brain regions communicate and work together during various tasks or at rest. Herein, the ICA approach is utilized to identify and extract the brain activation pattern in the brain of 24 control and 19 PTSD subjects in Phase 1, implemented in easily available GIFT software (<https://trendscenter.org/software/gift/>) (Allen et al., 2011). The preprocessed scans are used in group-level ICA. The group-level ICA is carried out by setting the value of component 25. Next, in ICA analysis the principal component analysis (PCA) is employed to reduce the data dimensionality and data de-noising and provides the booting for group-level ICA. Then, the reduced components were concatenated based on groups for the implementation of group-level ICA.

Second, to identify the most denoising components the Spatial base correlation between all subjects using the Default Mode Network (DMN) template was estimated to estimate the most relevant components (Patriat et al., 2016). The DMN in resting state networks (RSNs) is the most useful way to investigate the resting state network of the brain (Hu et al., 2016). The DMN concerning ICA is split into two parts such as anterior DMN and posterior DMN. The anterior DMN includes information on MPFC, dorsal MPFC, ACC, posterior cingulate cortex (PCC)/precuneus (PCu), anterior temporal lobe, inferior frontal gyrus, and lateral parietal cortex brain regions. The posterior DMN includes information on the posterior inferior parietal lobule, angular, hippocampal, and temporal lobe (Xu et al., 2016). Finally, ICA-Regression (ICA-R) is applied which is an effective method for investigating activation patterns between ICs extracted through ICA and regions-of-interest using the benefits of regression analysis. The detailed methodology of Phase 1 is given in Fig. 1. Two Sample t-tests is applied to know the activation pattern in the brain regions of PTSD and healthy control subjects.

2.3. 3D-CNN deep learning framework

In this study for Phase 2, we employed a 3D-CNN-based deep learning classification framework to classify PTSD subjects from healthy controls using ICA components. The framework was developed using the TensorFlow library. There were $(24+19) \times 80 = 3440$ rs-fMRI scans considered at the start of the experiment but after applying ICA it reduced to $(24+19) \times 25 = 1075$ unsorted components. Out of 25 unsorted ICA, the 10 ICAs selected for each subject of both PTSD and the control group based on correlation. The best-selected components $(24+19) \times 10 = 430$ for each group were further utilized in 3D-CNN analysis for the diagnosing process. The 430 3D-fMRI components or

images were split into 266, 114, and 50 images into training, validation, and testing sample parts, respectively, to use for classification purposes in 3D-CNN. To avoid the model from overfitting, we employed five-fold cross-validation in this work to report the mean accuracy of the model. The performance of 3D-CNN was evaluated through accuracy, ROC curve, 95 % AUC (area under the curve), sensitivity, specificity, false negative rate (FNR), false positive rate (FPR), precision, and confusion matrix.

Here, the 3D-CNN model for classification has the three general conventional categories of layers such as convolutional layers, pooling layers, and fully connected layers, which are mentioned in Fig. 2. In the input layer, the $79 \times 95 \times 79 \times 1$ shape of 3D components is considered as an input. At convolution layers first, second, and third the $32 - 3 \times 3 \times 3$, $64 - 3 \times 3 \times 3$, and $128 - 3 \times 3 \times 3$ filters were applied respectively. After every convolutional layer, $2 \times 2 \times 2$ pooling layers were added then flatten and dropout with 0.4. In the end, two dense layers were added with 128 and 1 unit respectively.

3. Analysis and results

The analysis and results of this study are based on the rs-fMRI 3D data of the 19 PTSD and 24 healthy control male subjects, who served in the Vietnam War. The preprocessed fMRI 3D data was converted to 3440 images. ICA is used to identify the best informative components for selected brain regions that communicate and work together during rest. To achieve the robustness and reproducibility of the 3D-CNN 5-fold cross-validation process has been used.

3.1. Brain activation extraction analysis

To identify the activation pattern in the preprocessed scans of PTSD and healthy control subjects the Spatial ICA (SICA) analysis is employed and performed on Group ICA of fMRI Toolbox (GIFT) in MATLAB 2018b. The 24 control and 19 PTSD subjects with preprocessed fMRI scans were imported into the GIFT toolbox individually and set the 25 number of ICA, respectively. Next, the Infomax algorithm has been employed to conduct IC analysis, creating the ICA components and time courses for both PTSD and healthy control subjects, respectively. The nosing components in the ICA were removed on the base of the correlation, as it is a useful approach (Griffanti et al., 2017). In this study, the ICA analysis is applied with a temporal method to obtain the most useful components on the base of correlation. The correlation was checked with the time courses of all subjects and DMN. ICs with higher correlation values indicate a stronger relevance to the DMN, while those below the threshold (correlation $\leq |0.60|$) were removed from further analysis, by ensuring that these are genuinely noise-related. Through this process, 10 out of 25 components were selected for both patient and control subjects based on correlation. The top 4 components out of 10 are arranged and

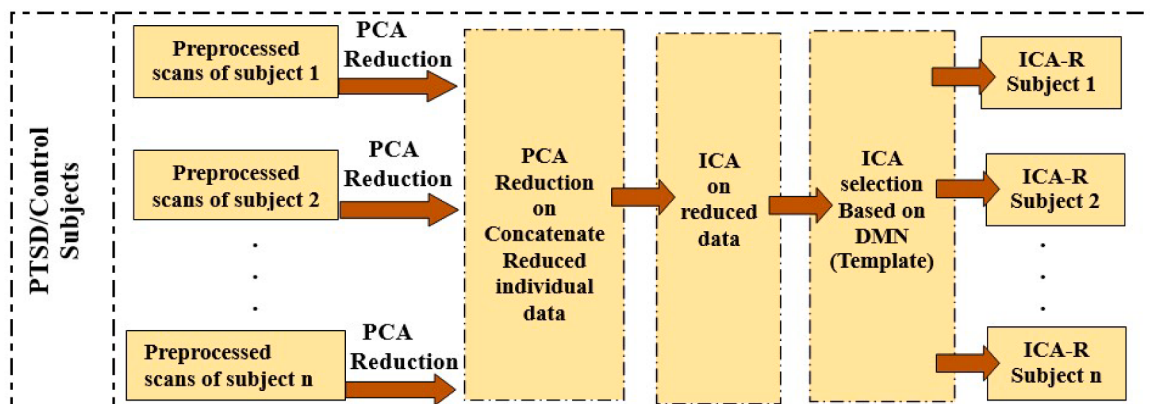


Fig. 1. Flowchart of the group-level ICA method for analysis of multi-subject fMRI data for Phase-1.

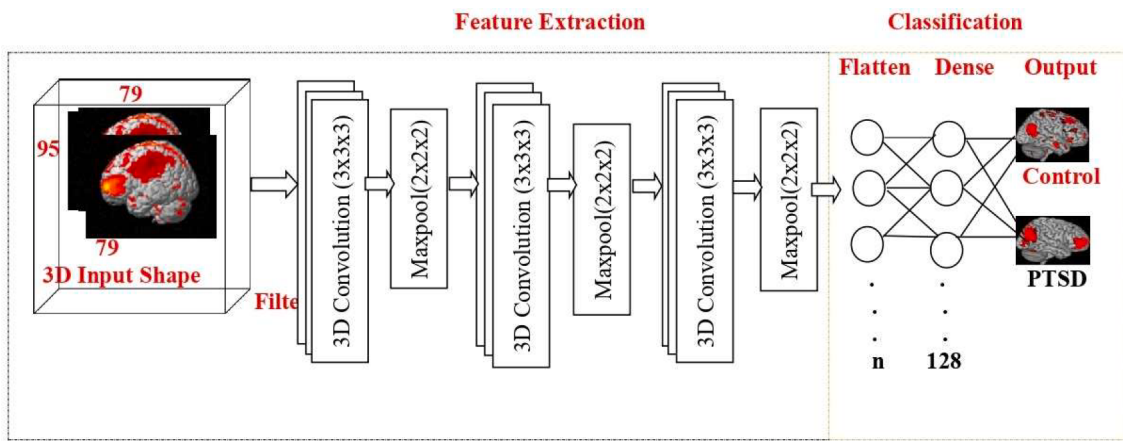


Fig. 2. Architecture of the 3D-CNN model for Phase 2.

the 20th, 22nd, 24th, and 25th components of healthy controls and the 12th, 17th, 24th and 25th components of PTSD are highlighted in Fig. 3.

The 10 selected components were further used in the second level analysis where we compared the mean activation levels between PTSD and the control group by carrying out the two-sample *t*-test. The *t*-statistic and *p*-values obtained to test the null hypothesis that there is no difference in activation levels between the two groups. The activation of PTSD subjects from control subjects is shown in Fig. 4, where blue to white color indicates negative to highly negative activation and from red to yellow indicates positive to highly positive activation. The positive and negative *t*-values indicate that the mean activation level and activation pattern in the regions-of-interest of PTSD subjects are higher and lower than the healthy control subjects, respectively. The regions-of-interest in this study are the hippocampus, insula, precuneus, amygdala, frontal superior medial, thalamus, para hippocampus, parietal inferior, ACC, angular gyrus, and supplement motor area. The most activated regions from the regions-of-interest in the brain of PTSD subjects are the amygdala and insula, as shown in Fig. 5. Conversely, decreased activation was observed in the hippocampus, precuneus, frontal superior medial, thalamus, par hippocampus, and inferior temporal cortex areas and displayed in Fig. 6.

3.2. Classification by machine learning techniques

As we have already applied the ICA to the preprocessed rs-fMRI data to decompose 3D fMRI data into a set of optimal independent

components. Then, the Principal Component Analysis (PCA) is employed for the dimensionality reduction of ICA components before applying Machine Learning (ML) techniques. The PCA created a lower-dimensional representation of ICA components, which are used as input features for ML techniques. In machine learning techniques the selected techniques such as Random Forest (RF), Naive Bayes (NB), Support vector machine (SVM), Decision tree (DT), K-nearest Neighbor (KNN), and Linear discriminant analysis (LDA) have been used in this study for the classification of PTSD and healthy control.

The same dimensioned features are categorized and labeled as "PTSD" or "Control" for classification aim. The finalized number of total features is split with a ratio of 62 % for training, 26 % for validation, and 12 % for testing. Therefore, the 430 features trifurcated into 266, 114, and 50 of the size of the sample for training, validation, and testing, respectively, for testing for PTSD classification than healthy control subjects.

All the applied ML techniques are evaluated on the basis of classification accuracy, Receiver Operating Characteristic (ROC) curve, and Area under the Curve (AUC). The ROC curve and AUC for each ML technique that is used to classify PTSD and healthy control subjects can be visualized in Fig. 7. Our analysis reveals that the ML models could not achieve precise results in both the training and testing phases, to distinguish between PTSD and healthy control subjects. Consequently, these inaccurate results lead us to not rely on these machine learning techniques and shift to any other better choice. Therefore, we made a transition from ML techniques to Deep Learning (DL) techniques and

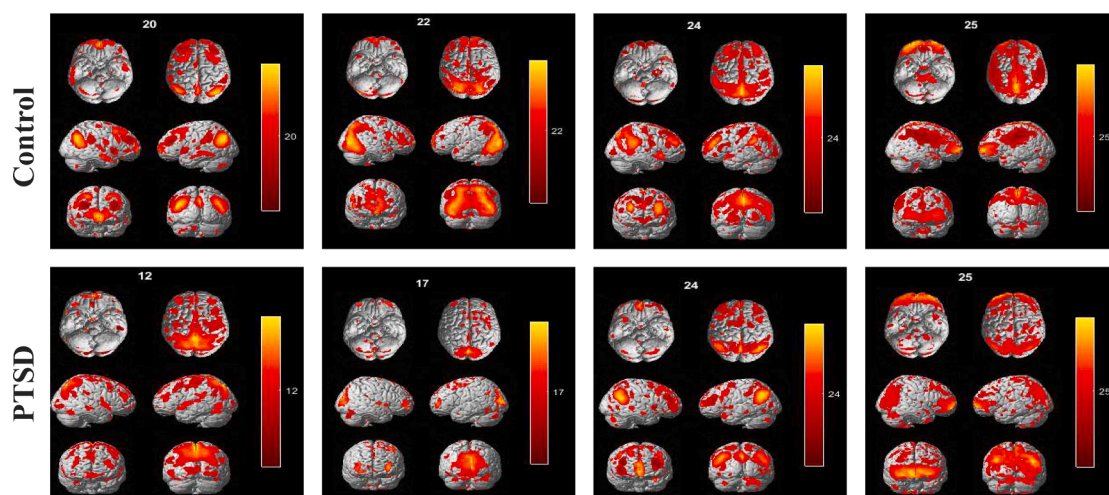


Fig. 3. The top 4 out of 10 highly correlated components related to DMN are highlighted in these brain images of both the PTSD and control subjects.

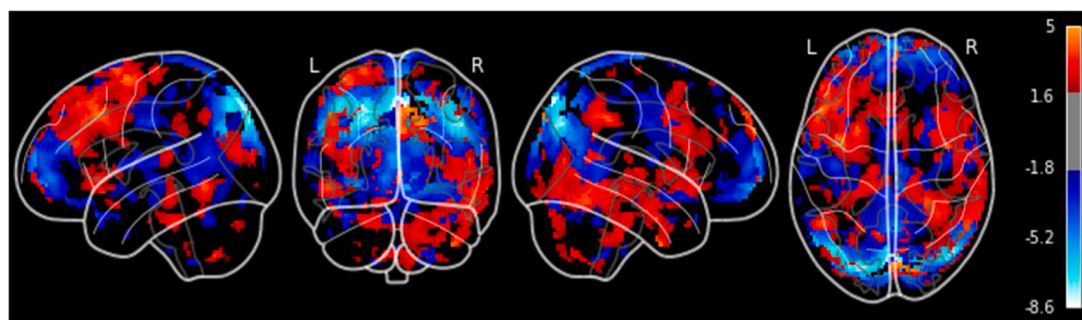


Fig. 4. Two sample *t*-tests between the whole brain regions of PTSD and healthy control subjects. The activation pattern is highlighted with blue and red colors. The blue color indicates negative activation in PTSD subjects than control and the red color presents positive activation in PTSD than control subjects.

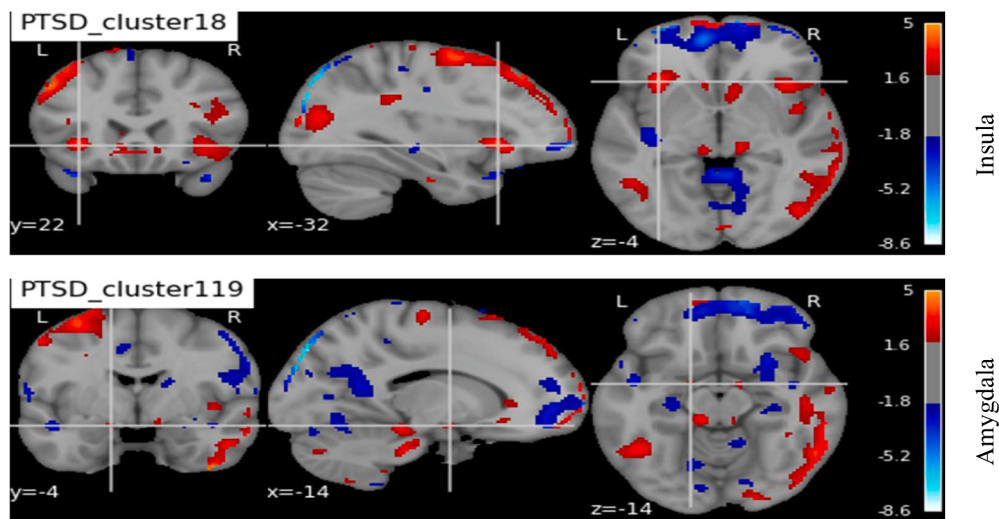


Fig. 5. The brain activation pattern of PTSD subjects with axial, coronal, and Sagittal view. The red color shows the positive activation concerning the insula and amygdala of PTSD subjects than control subjects.

adopted a 3D-CNN model to achieve the objective of the study more efficiently and accurately.

3.3. Classification by 3D-CNN

A five-fold cross-validated deep learning classification framework was implemented, using the 3D-CNN architecture in this study to identify PTSD and healthy control subjects. The intention of adopting 3D-CNN is to attain better results as compared to the ML techniques that are considered above in the analysis. The framework of the 3D-CNN was implemented on the TensorFlow library version 1.5 with Nvidia Quadro K1100M graphical processing unit (GPU) support. The architecture of the 3D-CNN is discussed in section 2.3 and presented in Fig. 2. The cross-validation is an extensively used technique for model evaluation. In the 5-fold cross-validation method dataset is split into five subsets, to train and evaluate the model five times, each time using a different subset as the test set and the remaining data as the training set. To assess model evaluation, to get a more accurate estimate, to reduce the risk of overfitting or underfitting, and to assess the stability and reliability performance of 3D-CNN across different data partitions.

In the goodness of fit criteria, the 3D-CNN model is also evaluated by observing accuracy and loss during each epoch and the results are presented in Fig. 8. By increasing the number of Epochs the accuracies have been approached to 1 and losses reduced to 0.001 approximately. The mean accuracy (loss) converges to 0.980 (0.015) for the training dataset and to 0.980 (0.016) for the validation dataset. The trend of these accuracies and losses indicates the model is well fitted on both datasets. The result of each fold of the 5-fold cross-validation of the 3D-CNN

model is given in Table 2.

To also test a trained and validated 3D-CNN model on a separate dataset that is entirely independent of the data used in the 5-fold cross-validation is considered a testing dataset. The performance of the 3D-CNN model concerning the accuracy, loss, ROC, AUC, sensitivity, specificity, FNR, FPR, precision and was also evaluated through confusion matrices and is displayed in Table 3. The averaged accuracy and loss with 5-fold cross-validation of training data were 98.00 %, and 0.015, respectively. Similarly, the averaged accuracy and loss with 5-fold cross-validation of validation data have been achieved as 97.98 %, and 0.016, respectively. The values of AUC close to one suggest that the 3D-CNN has a strong discriminatory ability and its close range indicates that the model's performance is highly consistent across different folds and data subsets. The ROC curves in Fig. 9 touched the upper left corner, it is due to the high accuracy of 98.00 % or above of the 3D-CNN model. A ROC curve that quickly rises to the upper left corner of the plot is the result of consistently high sensitivity and very low FPRs. This indicates that the model produces a low error when differentiating between the PTSD and healthy control subjects. Therefore, the AUCs are close to 1.0. This is the reason the ROC curves are not very obvious. Additionally, the high values of sensitivity and specificity indicate that the model is very good at correctly identifying PTSD or healthy control subjects and is very good at correctly identifying individuals without a specific condition. Similarly, the values of FNR, FPR, precision, and confusion matrices reveal that the 3D-CNN has excellent discriminatory power.

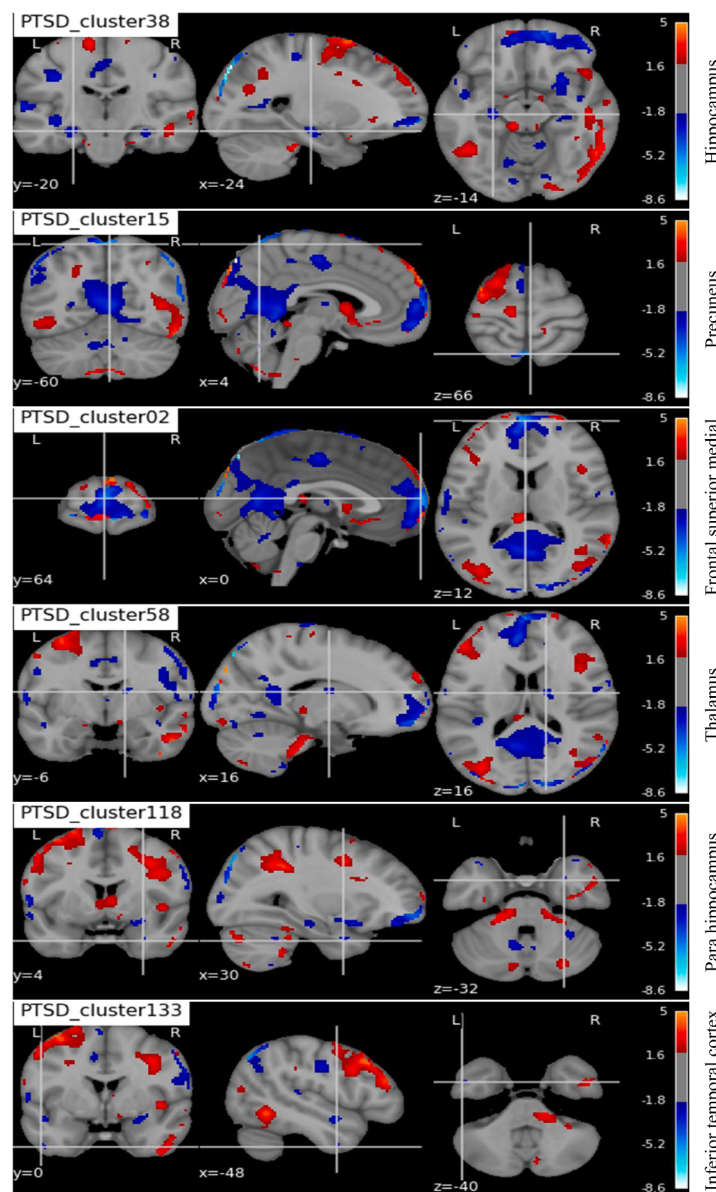


Fig. 6. The ROI-based brain activation pattern of PTSD subjects present in axial, coronal, and sagittal views of the brain. The blue color shows the negative activation of PTSD subjects concerning the Hippocampus, precuneus, Frontal superior medial, Thalamus, Para hippocampus, and Inferior temporal cortex than control subjects.

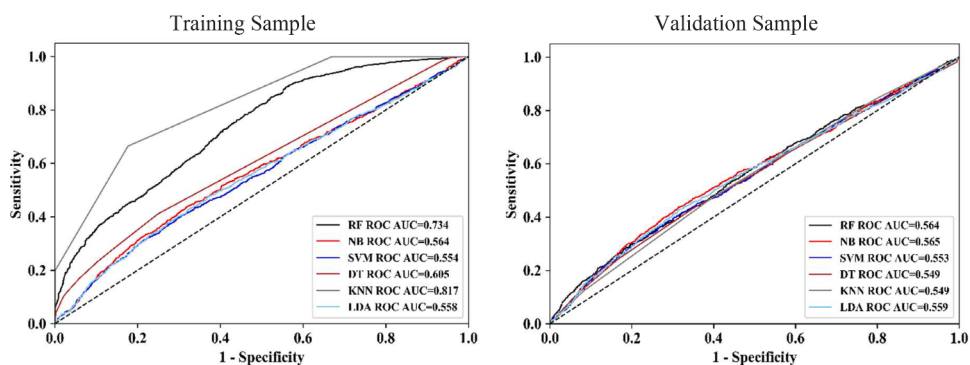


Fig. 7. The sensitivity analysis based on ROC and AUC of all ML models. The ROC and AUC represent the degree of separability or classification of PTSD from control subjects of all ML models. The black, red, blue, brown, gray, and sky-blue lines explained the performance of RF, NB, SVM, DT, KNN, and LDA respectively.

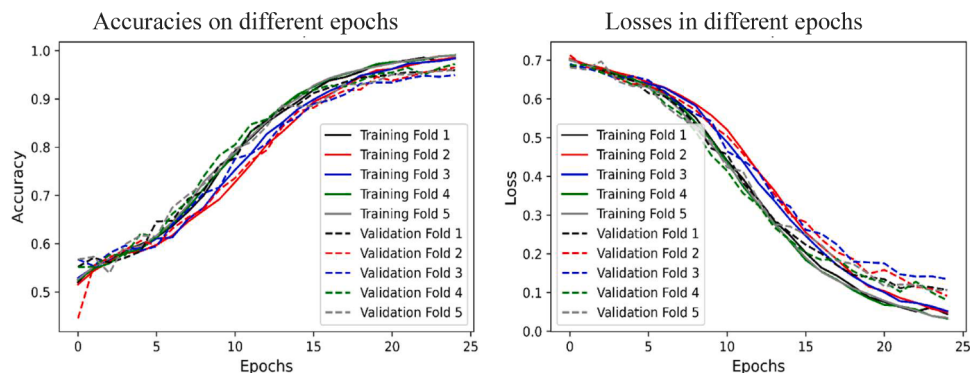


Fig. 8. The 3D-CNN Model based on accuracies and losses under 25 epochs using the 5-fold cross-validation method. Where solid lines present the accuracies and losses of training data and dashed lines present the accuracies and losses of validation data. The black, red, blue, green, gray solid, and dashed lines present accuracy and loss of fold 1, fold 2, fold 3, fold 4, and fold 5 respectively.

Table 2
The losses and accuracies with a 5-fold cross-validation approach of training and testing dataset.

Dataset	Metric	fold-1	fold-2	fold-3	fold-4	fold-5	Mean
Training	Accuracy	0.981	0.976	0.983	0.979	0.981	0.980
	Loss	0.017	0.016	0.018	0.010	0.012	0.015
Validation	Accuracy	0.987	0.964	0.987	0.985	0.976	0.980
	Loss	0.017	0.017	0.018	0.016	0.011	0.016

Table 3
Evaluation of the 3D-CNN classification ability with different goodness of fit metrics.

Metrics	Training	Validation	Testing
Accuracy	98.12 %	98.25 %	98.00 %
Loss	0.073	0.064	0.075
AUC[CI-95 %]	0.99 [0.998 - 0.999]	0.98 [0.972 - 0.990]	0.99[0.979 - 1.00]
Sensitivity	97.66 %	98.46 %	96.15 %
Specificity	98.55 %	97.97 %	100 %
FNR	0.023	0.015	0.038
FPR	0.014	0.020	0.001
Precision	100 %	98.46 %	100 %
Confusion matrix	$\begin{bmatrix} 125 & 2 \\ 3 & 136 \end{bmatrix}$	$\begin{bmatrix} 64 & 1 \\ 1 & 48 \end{bmatrix}$	$\begin{bmatrix} 25 & 0 \\ 1 & 24 \end{bmatrix}$

4. Discussion and conclusion

In this study, we have discussed two significant contributions to the automated diagnosis of PTSD. First, we utilized the machine learning techniques and second, we adopted a 3D-CNN deep learning architecture for classification on the base of 3D-ICA components. To apply the

ICA analysis with a temporal method to obtain the most useful components on the base of correlation. These 3D-ICA components are further used for classification procedures using the 3D-CNN model. To date, best of our knowledge, it is the first time 3D-CNN has been used in this way to distinguish patients with PTSD from healthy controls. As a result, we have achieved superior classification results through 3D-CNN as compared to the machine learning-based classifications. In our previous work (Shahzad et al., 2021), we classified PTSD and healthy control subjects with ANN and obtained 95 % accuracy through the first-level analysis only, which was not as sophisticated as the current analysis. However, the analysis in this study is more advanced as after the pre-processing, the ICA is applied, and obtained the best components that are used in statistical analysis and achieved more precise results. Therefore, this method supersedes the other previous analysis method, including our own previous work (Shahzad et al., 2021; Saba et al., 2022). To date, three studies have been reported that classify PTSD and healthy controls using deep learning and fMRI (Liu et al., 2015; Shahzad et al., 2021; Saba et al., 2022).

The brain regions activation and connectivity pattern have been used to classify healthy controls and individuals with PTSD. Several studies have explored this classification task using rs-fMRI data. Zhu et al. (Zhu et al., 2020) employed multivariate pattern analysis with a relevance vector machine to achieve a diagnostic accuracy of 89.2 % in distinguishing PTSD patients from trauma-exposed healthy controls based on large-scale brain network connectivity. (Liu et al., 2015) recruited twenty motor vehicle accidental patients with PTSD and twenty healthy controls and obtained 92.5 % classification accuracy by SVM with an integrated mixed-kernel matrix.

Many rs-fMRI studies have reported abnormalities in PTSD sufferers' brain regions. The most commonly stated and our regions-of-interest in this study are the hippocampus, insula, precuneus, amygdala, frontal superior medial, thalamus, para hippocampus, parietal inferior, ACC, angular gyrus, and supplement motor area. Taking the preprocessed

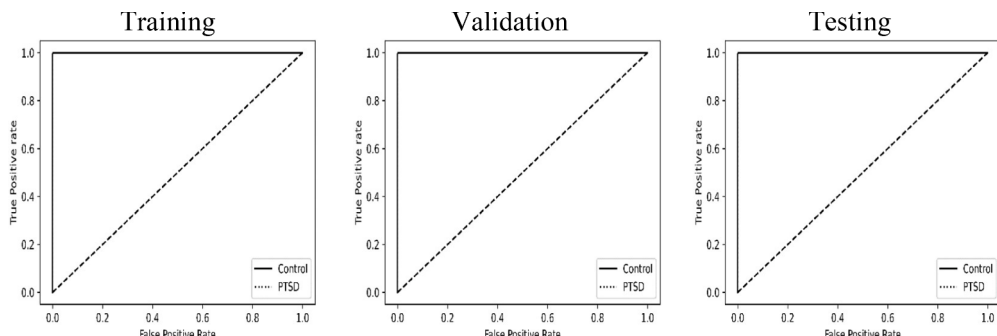


Fig. 9. The ROC represents the sensitivity analysis of the 3D-CNN Model in the classification of PTSD from control subjects.

scans, we completed our investigation into two Phases, in the first Phase the reliable components nominated using the ICA with DMN on the base of correlation and activation pattern with *t*-test. In Phase 2 the ML and DL approaches were utilized for PTSD classification purposes. The identified activation pattern in the regions-of-interest of the PTSD subjects mostly matches with literature, as displayed in Fig. 5 and Fig. 6. More specifically, the increased activation was observed in the amygdala, and insula (Joshi et al., 2020; Yan et al., 2013) and the regions where decreased activation was noticed in the MPFC, Hippocampus, precuneus, thalamus, Para hippocampus, and inferior parietal cortex (Francati et al., 2007; Joshi et al., 2020; Yan et al., 2013).

In Phase 2, we classified the components obtained in Phase 1 of PTSD and healthy control subjects by applying ML and DL techniques. In ML techniques the considered techniques were RF, NB, SVM, DT, KNN, and LDA and in DL techniques 3D-CNN was used to classify PTSD and healthy control. All of the ML models under consideration have been applied using the components selected by the PCA approach, and their suitability for PTSD subject identification has been tested using various ways. According to the training and validation datasets, the AUC of the RF, NB, SVM, DT, KNN, and LDA has been obtained at 0.73, 0.56, 0.55, 0.60, 0.82, 0.55, and 0.56, 0.56, 0.55, 0.54, 0.54, and 0.55, respectively. In the training, validation, and testing dataset, the outcomes of ICA-based 3D-CNN exhibit great accuracy as compared to considered ML models. The 3D-fMRI scans of PTSD and control individuals were correctly classified in 261, 112, and 49 scans, while 5, 2, and 1 cases were wrongly classified as mentioned in the confusion matrices that are given in Table 3. In training, validation, and testing data, the 3D-CNN achieved accuracy scores of 98.12 %, 98.25 %, and 98.00 %, respectively.

All the considered goodness-of-fit criteria, such as sensitivity, specificity, the FNR, FPR, ROC with the area under the curve (AUC), precision, accuracy, and 5-fold cross-validation accuracies collectively indicate that the proposed 3D-CNN model is well-fitted and suitable for classifying PTSD subjects using their 3D-fMRI scans. In the fMRI investigations for classification, K-fold cross-validation is useful because it enables model selection and classifier error estimation (White and Power, 2023). Our 3D-CNN approach efficiently distinguishes between PTSD and control subjects, providing valuable insights into brain region activation patterns and enabling the identification of PTSD subjects among control subjects. These findings offer valuable support for future researchers to study the PTSD brain by focusing the brain regions those highlighted here.

Statements and declarations

Data used in preparation of this article were obtained from the Alzheimer's Disease Neuroimaging Initiative (ADNI) database (adni.loni.usc.edu). As such, the investigators within the ADNI contributed to the design and implementation of ADNI and/or provided data but did not participate in the analysis or writing of this report. A complete listing of ADNI investigators can be found at: http://adni.loni.usc.edu/wp-content/uploads/how_to_apply/ADNI_Acknowledgement_List.pdf. This study was approved by the Department of Statistics at the University of Gujarat, Gujarat, Pakistan.

This research received no specific grant from any funding agency in the public, commercial, or not-for-profit sectors. The authors conducted this study without external financial support.

The authors declare that there are no conflicts of interest regarding the publication of this manuscript.

CRediT authorship contribution statement

Mirza Naveed Shahzad: Writing – review & editing, Writing – original draft, Visualization, Validation, Supervision, Resources, Methodology, Investigation, Formal analysis, Data curation, Conceptualization. **Haider Ali:** Writing – original draft, Validation, Methodology,

Investigation, Formal analysis.

Declaration of competing interest

The authors confirm that there are no known conflicts of interest associated with this publication and there has been no significant financial support for this work that could have influenced its outcome.

References

- Abbas, S.Q., Chi, L., Chen, Y.-P.P., 2023. Transformed domain convolutional neural network for Alzheimer's disease diagnosis using structural MRI. *Pattern Recognit.* 133, 109031.
- Agarwal, D., Berbís, M.Á., Luna, A., Lipari, V., Ballester, J.B., de la Torre-Diez, I., 2023. Automated medical diagnosis of Alzheimer's disease using an efficient net convolutional neural network. *J. Med. Syst.* 47, 57.
- Allen, E.A., Erhardt, E.B., Damaraju, E., et al., 2011. A baseline for the multivariate comparison of resting-state networks. *Front Syst. Neurosci.* 5, 2.
- Bandettini, P.A., 2012. Twenty years of functional MRI: the science and the stories. *NeuroImage* 62, 575–588.
- Bruce, S.E., Buchholz, K.R., Brown, W.J., Yan, L., Durbin, A., Sheline, Y.I., 2013. Altered emotional interference processing in the amygdala and insula in women with post-traumatic stress disorder. *NeuroImage: Clinical* 2, 43–49.
- Canario, E., Chen, D., Biswal, B., 2021. A review of resting-state fMRI and its use to examine psychiatric disorders. *Psychoradiology* 1, 42–53.
- Chen, L., Xia, C., Sun, H., 2020. Recent advances of deep learning in psychiatric disorders. *Precis. Clinical Med.* 3, 202–213.
- Christova, P., James, L.M., Engdahl, B.E., Lewis, S.M., Georgopoulos, A.P., 2015. Diagnosis of posttraumatic stress disorder (PTSD) based on correlations of prewhitened fMRI data: outcomes and areas involved. *Exp. Brain Res.* 233, 2695–2705.
- Dipasquale, O., Griffanti, L., Clerici, M., Nemni, R., Baselli, G., Baglio, F., 2015. High-dimensional ICA analysis detects within-network functional connectivity damage of default-mode and sensory-motor networks in Alzheimer's disease. *Front. Hum. Neurosci.* 9, 43.
- Fox, M.D., Greicius, M., 2010. Clinical applications of resting state functional connectivity. *Front Syst Neurosci* 4, 1443.
- Francati, V., Vermetten, E., Bremner, J.D., 2007. Functional neuroimaging studies in posttraumatic stress disorder: review of current methods and findings. *Depress. Anxiety* 24, 202–218.
- Galovski, T., Lyons, J.A., 2004. Psychological sequelae of combat violence: a review of the impact of PTSD on the veteran's family and possible interventions. *Aggress. Violent Behav* 9, 477–501.
- Griffanti, L., Douaud, G., Bijsterbosch, J., et al., 2017. Hand classification of fMRI ICA noise components. *NeuroImage* 154, 188–205.
- Hu, Y., Wang, J., Li, C., Wang, Y.-S., Yang, Z., Zuo, X.-N., 2016. Segregation between the parietal memory network and the default mode network: effects of spatial smoothing and model order in ICA. *Sci. Bulletin* 61, 1844–1854.
- Hughes, K.C., Shin, L.M., 2011. Functional neuroimaging studies of post-traumatic stress disorder. *Expert. Rev. Neurother.* 11, 275–285.
- Investigators, E.M., Alonso, J., Angermeyer, M., et al., 2004. Prevalence of mental disorders in Europe: results from the European Study of the Epidemiology of Mental Disorders (ESEMeD) project. *Acta Psychiatr. Scand.* 109, 21–27.
- Jiao, L., Wu, H., Bie, R., Umek, A., Kos, A., 2018. Multi-sensor golf swing classification using deep CNN. *Procedia Comput. Sci.* 129, 59–65.
- Joshi, S.A., Duval, E.R., Kubat, B., Liberon, I., 2020. A review of hippocampal activation in post-traumatic stress disorder. *Psychophysiology* 57, e13357.
- Ke, J., Zhang, L., Qi, R., et al., 2016. A longitudinal fMRI investigation in acute post-traumatic stress disorder (PTSD). *Acta Radiol.* 57, 1387–1395.
- Kessler, R.C., Berglund, P., Demler, O., Jin, R., Merikangas, K.R., Walters, E.E., 2005. Lifetime prevalence and age-of-onset distributions of DSM-IV disorders in the National Comorbidity Survey Replication. *Arch. Gen. Psychiatry* 62, 593–602.
- Liu, F., Xie, B., Wang, Y., et al., 2015. Characterization of post-traumatic stress disorder using resting-state fMRI with a multi-level parametric classification approach. *Brain. Topogr.* 28, 221–237.
- Logothetis, N.K., 2008. What we can do and what we cannot do with fMRI. *Nature* 453, 869–878.
- Mikl, M., Mareček, R., Hluštík, P., et al., 2008. Effects of spatial smoothing on fMRI group inferences. *Magn. Reson. Imaging* 26, 490–503.
- Nichols, T.E., Das, S., Eickhoff, S.B., et al., 2017. Best practices in data analysis and sharing in neuroimaging using MRI. *Nat. Neurosci.* 20, 299–303.
- Norman, K.A., Polyn, S.M., Detre, G.J., Haxby, J.V., 2006. Beyond mind-reading: multi-voxel pattern analysis of fMRI data. *Trends Cogn. Sci. (Regul. Ed.)* 10, 424–430.
- Oh, J., Chun, J.W., Kim, E., Park, H.J., Lee, B., Kim, J.J., 2017. Aberrant neural networks for the recognition memory of socially relevant information in patients with schizophrenia. *Brain. Behav.* 7, e00602.
- Patriat, R., Birn, R.M., Keding, T.J., Herrings, R.J., 2016. Default-mode network abnormalities in pediatric posttraumatic stress disorder. *J. Am. Acad. Child & Adolescent Psych.* 55, 319–327.
- Qureshi, M.N.I., Oh, J., Cho, D., Jo, H.J., Lee, B., 2017. Multimodal discrimination of schizophrenia using hybrid weighted feature concatenation of brain functional connectivity and anatomical features with an extreme learning machine. *Front. Neuroinform* 11, 59.

- Saba, T., Rehman, A., Shahzad, M.N., Latif, R., Bahaj, S.A., Alyami, J., 2022. Machine learning for post-traumatic stress disorder identification utilizing resting-state functional magnetic resonance imaging. *Microsc. Res. Tech.* 85, 2083–2094.
- Shahzad, M.N., Ali, H., Saba, T., Rehman, A., Kolivand, H., Bahaj, S.A., 2021. Identifying patients with PTSD utilizing resting-state fMRI data and neural network approach. *IEEE Access* 9, 107941–107954.
- Shirer, W.R., Ryali, S., Rykhlevskaia, E., Menon, V., Greicius, M.D., 2012. Decoding subject-driven cognitive states with whole-brain connectivity patterns. *Cereb. Cortex* 22, 158–165.
- Sivarajini, S., Sujatha, C., 2020. Deep learning based diagnosis of Parkinson's disease using convolutional neural network. *Multimed Tools Appl* 79, 15467–15479.
- Sladky, R., Friston, K.J., Tröbstl, J., Cunningham, R., Moser, E., Windischberger, C., 2011. Slice-timing effects and their correction in functional MRI. *Neuroimage* 58, 588–594.
- Smith, M.W., Schnurr, P.P., Rosenheck, R.A., 2005. Employment outcomes and PTSD symptom severity. *Ment. Health Serv. Res.* 7, 89–101.
- Watkins, L.E., Sprang, K.R., Rothbaum, B.O., 2018. Treating PTSD: a review of evidence-based psychotherapy interventions. *Front. Behav. Neurosci.* 12, 258.
- Weiner, M.W., Harvey, D., Hayes, J., et al., 2017. Effects of traumatic brain injury and posttraumatic stress disorder on development of Alzheimer's disease in Vietnam veterans using the Alzheimer's Disease Neuroimaging Initiative: preliminary report. *Alzheimer's & Dementia: Translat. Res. Clinical Intervent.* 3, 177–188.
- White, J., Power, S.D., 2023. k-Fold cross-validation can significantly over-estimate true classification accuracy in common EEG-Based Passive BCI Experimental Designs: an empirical investigation. *Sensors* 23, 6077.
- Xu, X., Yuan, H., Lei, X., 2016. Activation and connectivity within the default mode network contribute independently to future-oriented thought. *Sci. Rep.* 6, 21001.
- Yan, X., Brown, A.D., Lazar, M., et al., 2013. Spontaneous brain activity in combat related PTSD. *Neurosci. Lett.* 547, 1–5.
- Yen, C., Lin, C.-L., Chiang, M.-C., 2023. Exploring the frontiers of neuroimaging: a review of recent advances in understanding brain functioning and disorders. *Life* 13, 1472.
- Zhu, H., Yuan, M., Qiu, C., et al., 2020. Multivariate classification of earthquake survivors with post-traumatic stress disorder based on large-scale brain networks. *Acta Psychiatr. Scand.* 141, 285–298.
- Zhu, Z., Huang, X., Du, M., et al., 2023a. Recent advances in the role of miRNAs in post-traumatic stress disorder and traumatic brain injury. *Mol. Psychiatry* 28, 2630–2644.
- Zhu, X., Kim, Y., Ravid, O., et al., 2023b. Neuroimaging-based classification of PTSD using data-driven computational approaches: a multisite big data study from the ENIGMA-PGC PTSD consortium. *Neuroimage* 283, 120412.